Δελτίο της Ελληνικής Γεωλογικής Εταιρίας τομ. XXXII/1, 97-104, 1998 Bulletin of the Geological Society of Greece vol. XXXII/1, 97-104, 1998
Πρακτικά 8ου Διεθνούς Συνεδρίου, Πάτρα Μάιος 1998 Proceedings of the 8th International Congress, Patras, May 1998

EXHUMATION OF BLUESCHISTS FROM SAMOS ISLAND, GREECE

U. RING[1]

ABSTRACT

In this contribution I quantify to a first order the amounts which horizontal extension, vertical ductile thinning and erosion contributed to the ~50 km of exhumation of the blueschists exposed on Samos Island. Eocene to Early Oligocene horizontal crustal shortening caused thrusting of the blueschists onto a low-grade foreland unit (Kerketas nappe). We estimate that vertical ductile thinning associated with a subhorizontal foliation contributed ~9-10 km of exhumation in the hangingwall during thrusting. The remaining ~15-16 km of exhumation must have been achieved by erosion at an inferred average rate of ~0.8 mm/a. Horizontal crustal extension probably commenced in mid-Oligocene times and continued intermittently until the present. The throw on extensional faults during this phase accounts for ≤15-16 km of blueschist exhumation. Ductile thinning contributed another ~2-3 km. Present-day erosion rates are on the order of 0.2 mm/a. Extrapolating this rate back into the mid Oligocene yields 6 km of erosional exhumation since then.

KEY WORDS: Aegean, Samos Island, Tectonics, Metamorphism, Erosion, Exhumation

1. INTRODUCTION

We aim to quantify the relative contributions which the three agents of exhumation-erosion, ductile flow and horizontal extension (Brandon & Ring 1997)-contributed to the total exhumation of the blueschists exposed on Samos Island, Greece. It is widely believed that exhumation of Aegean blueschists is chiefly due to horizontal extension (Lister et al. 1984). Indeed, a number of Early Miocene to Recent extensional shear zones and normal faults have been mapped in the Aegean Islands (e.g. Avigad & Garfunkel 1991, Buick 1991). Nonetheless, little is known on the throw on those extensional structures and thus the contribution that horizontal extension has made to the total exhumation is hard to assess. Furthermore, the onset of well-constrained extensional deformation is not well known but certainly postdates the Eocene peak of high-P metamorphism considerably. A penetrative subhorizontal foliation and stretching lineation provide evidence that subhorizontal ductile flow is an important process that contributed to the exhumation of the blueschists. The huge volumes of Tertiary to Recent sediment in the Pindos and Westhellenic units, in the Aegean Sea and in onland grabens indicate that erosion also aided exhumation.

2. SETTING

The Cycladic Massif and the Menderes Massif (CMM) form an arcuate orogen to the north of the present-day active margin which marks the site of northeastwards subduction of the African plate beneath the Apulian-Anatolian microplate. The CMM consists of a stack of tectonic units which are interpreted as forming a pile of nappes. In ascending order these are: (1) The *Basal Unit* composed of a thick sequence of dolomitic marble. (2) The *Blueschist Unit* comprising a basement of pre-Permian ortho- and paragneiss overlain by a shelf sequence of marble, metapelite, quartzite and metabasite (Jansen 1977). Above this shelf sequence is a melange-like assemblage made up of ophiolitic rocks and garnet-mica schist embedded

[1] Institut für Geowissenschaften, Universität Mainz, 55099 Mainz, Germany

in a shaly matrix (Erdogan & Güngör 1992) (Fig.1). (3) The *Upper Unit* consists of three subunits: (*i*) The composite ophiolite nappe composed of unmetamorphosed ophiolitic rocks and low-pressure/high-temperature metamorphic rocks of Late Cretaceous age (Seidel et al. 1981). (*ii*) The Late Cretaceous to Paleogene Vardar-Izmir-Ankara suture zone which fringes the CMM to the north. (*iii*) The Lycian nappes to the southeast which are dominantly made up by relatively unmetamorphosed carbonate successions capped by Eocene to Oligocene clastic rocks (Collins & Robertson 1997). (4) Sedimentary basins filled with continental (in the north) and marine (in the south) Miocene and younger molasse-type sediments (Jansen 1977).

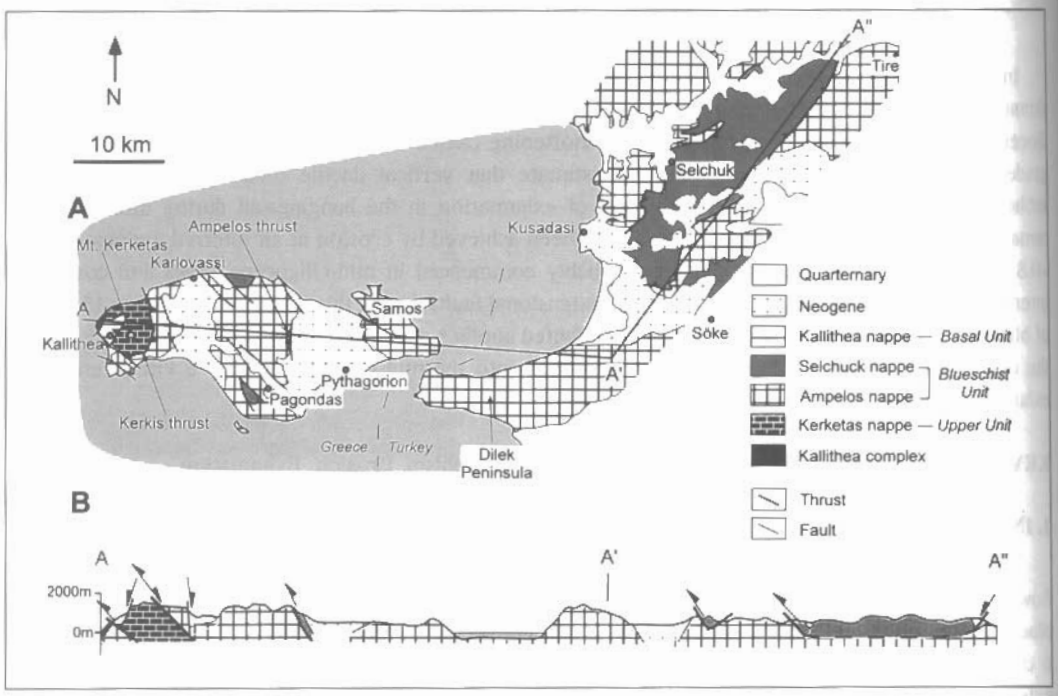

Fig. 1: Tectonic map (a) and cross section (b) of Samos Island and adjacent Dilek Peninsula showing general nappe structure (after Theodoropoulos 1979; Papanikolaou 1979; Erdogan & Güngör 1992; and our own detailed mapping) (vertical exaggeration of cross section is 2:1). A major metamorphic hiatus occurs between the unmetamorphosed Kallithea nappe (as part of the composite opiolite nappe) and the underlying greenschist-facies Kerketas nappe. Prograde metamorphic discontinuities occur across the Kerkis and Ampelos thrusts. Note late top-W displacing fault in westermost part of cross section which brings the Kerketas nappe onto the Kallithea complex.

Our mapping at the 1:10,000 scale over the last three years on Samos Island augmented the work of Theodoropoulos (1979) and Papanikolaou (1979) and revealed that the nappe stack (Fig.1) consists of six major tectonic units. In ascending order they are: (A) The Kallithea complex consisting of dolomitic and slicious marble, calc-silicate rock and amphibolite (Theodoropoulos 1979). (B) The Kerketas nappe of the *Basal Unit* which is made up of at least 1000 m thick succession of monotonous dolomitic marble, the base of which is not exposed. (C) The Ampelos nappe made up of marble, metapelite, quartzite, metagranite and metabasite and, (D) the Selühuk nappe. The Selühuk nappe contains metagabbro, in part in primary contact with serpentinized peridotite, and garnet-mica schist. The Ampelos and the Selühuk nappes belong to the *Blueschist Unit*. (E) The Kallithea nappe, as part of the composite ophiolite nappe of the *Upper Unit*, consists of peridotite, basalt, Triassic-Jurassic limestone, radiolarite and sandstone (Theodoropoulos 1979). (F) Fluviatile to lacustrine, molasse-type sediments were deposited in the Miocene in N-, NE- and WNW-oriented graben[illegible] sedimentation which

prevailed until about 8 Ma when fluviatile conglomerates were deposited which are in turn overlain by lacustrine sediment (Weidmann et al. 1984). At present, Samos Island has a very rugged topography with local relief reaching values on the order of 1.5 km.

3. METAMORPHISM

Estimates for blueschist-facies P-T conditions (M_1) in the Ampelos nappe are 420-490°C and 11-13 kbar (Chen 1992) (Fig.2). For the Selühuk nappe, Mposkos & Perdikatsis (1984) report glaucophane gabbro and omphacitic rock and Chen (1992) estimated ~550°C and >12 kbar for garnet-mica schist on Samos. For the Kerketas nappe, no evidence for blueschist-facies metamorphism exists; the same is true for weakly metamorphosed marbles of the *Basal Unit* on the islands of Tinos (Katzir et al. 1996) and Evia (Katsikatsos 1977).

Decompression led to growth of barroisite from glaucophane. This transition from blueschist- to greenschist-facies conditions occurred at pressures of between 6.5 and 7.5 kbar (Chen 1992). A subsequent Barrovian-type metamorphic overprint in the Ampelos and Selühuk nappes reached temperatures of about 450°C (Chen 1992). Our work indicates that decompression and cooling led to the formation of phengite (Si=≤3.36 pfu), paragonite, chlorite, garnet$_2$ (Alm_{70-77}, Grs_{18-23}), albite$_2$ and epidote$_2$ from glaucophane, kyanite, chloritoid, garnet$_1$ (Alm_{56-62}, Grs_{24-29}), albite$_1$ and epidote$_1$. Phengite barometry yields a minimum pressure of 6-7 kbar at 380°C which is in accord with the pressure estimate of Chen (1992) for the blueschist/greenschist transition. This M_2 decompression/ cooling assemblage was then replaced by biotite, chlorite, muscovite, phengite (Si=≤3.24 pfu) garnet$_3$ (Alm_{56-68}, Grs_{8-15}), albite$_3$ and epidote$_3$ during further decompression but increasing temperature (M_3). Phengite barometry yielded 4-5 kbar at 450°C. The occurrence of both corundum and diaspore in metabauxite of the Kerketas nappe indicate temperatures of about 400-450°C at 3-5 kbar. The Kallithea nappe was not affected by regional metamorphism.

The data indicate metamorphic breaks across the nappe pile (Fig.2). P-T conditions increase abruptly across the Kerkis thrust and slightly across the Ampelos thrust. Both thrusts put higher-pressure rocks onto lower-pressure rocks. Since the post-blueschist-facies overprint affected the entire nappe pile without major discontinuities (Chen 1992), we conclude that the metamorphic breaks formed prior to M_2. For the Kerkis thrust, the data indicate a pressure gap of about 6-9 kbar, equivalent to at least 20-30 km of crust. The tectonic contact between the Kallithea nappe and the underlying nappes (Fig.1) is characterized by an inverse metamorphic break which postdates the M_3 metamorphism. According to Avigad & Garfunkel (1991), the composite ophiolite nappe on Tinos was finally emplaced above the underlying units before 18 Ma. The final emplacement of this ophiolite nappe is generally attributed to horizontal crustal extension (Lister et al. 1984). Based on the P-T data (Fig.2), we suggest that the extensional emplacement of the Kallithea nappe caused a barometric discontinuity of ≤4 kbar, equivalent to ≤14 km of missing crust.

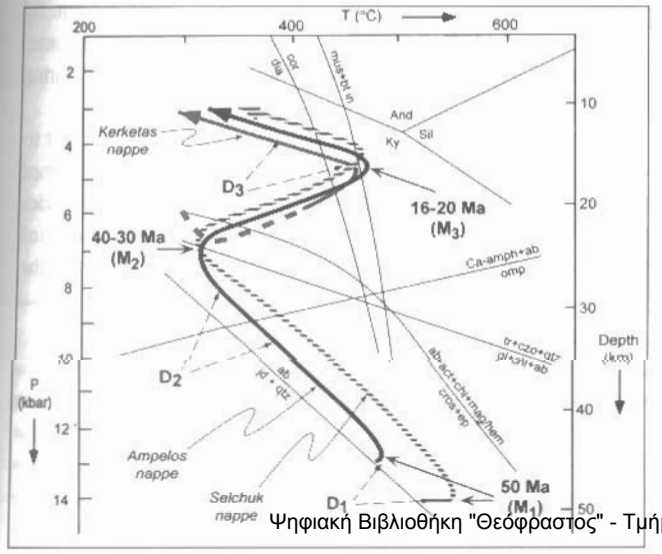

Fig. 2: P-T-t paths for the different nappes. *Note that Kallithea nappe (not shown) was* emplaced late when all nappes reached relatively shallow crustal levels. Age constraints are from Altherr et al. (1979) and Wijbrans et al. (1990). The barometric data are converted to depth assuming an average rock density of 2.8 g/cm^3.

No geochronologic data exist for Samos Island. Nonetheless, age data for the *Blueschist Unit* for a number of island (Sifnos, Naxos, Ios, Syros, Tinos, Ikaria) across the entire Aegean are remarkably similar and are interpreted to date the peak of high-pressure metamorphism at about 50 Ma (Altherr et al. 1979; Wijbrans et al. 1990). Cooling below ~350°C took place between 30-40 Ma and the Barrovian-type overprint occurred at about 16-20 Ma (Wijbrans et al. 1990) concurrent with a pulse of calc-alkaline magmatism (Fig.2).

The shape of the P-T-t path in Fig.2 illustrates a major change in the thermal structure at ~30 Ma. The onset of high-pressure metamorphism in Crete at about 25 Ma (Altherr et al. 1979) is younger than that of the Aegean. Hence, we correlate this major thermal transition to initial retreat of the subducting slab. Asthenospheric backflow associated with slab retreat may have triggered the voluminous Miocene magmatism and increased mantle heat flow may have caused the M_3 metamorphism. Since extensional deformation is commonly linked to slab retreat (Lister et al. 1984, Buick 1991), horizontal crustal extension is inferred to have started already during the Oligocene, i.e. at about 30 Ma.

4. DEFORMATION

We recognised two generations of ductile structures (D_1 and D_2) related to the blueschist- and transitional blueschist/greenschist-facies metamorphism. D_1 and D_2 are separated by a porphyroblastic stage of blueschist-facies metamorphism. Associated kinematic indicators include (1) asymmetric strain shadows around $garnet_{1/2}$ containing glaucophane, barroisite and chloritoid; (2) rotated glaucophane and (3) asymmetries of $D_{1/2}$ isoclinal folds. Indicators are scarce and do not provide a consistent sense of shear; however, the majority of the data is consistent with the data of Ridley (1984) from Syros Island indicating top-SE thrusting. At the same time as thrusting was going on in deep levels, the Lycian cover nappes were also thrust towards the SE as recorded by the development of an Eocene-Oligocene flexural foreland basin (Collins & Robertson 1997). Deformation/ crystallisation relationships and the P-T data show that the nappe pile consisting of the Kerketas-, Ampelos- and Selühuk nappes was assembled during D_2.

The Kerkis thrust was strongly overprinted by top-E kinematic indicators (D_3). The overall geometric relationship between the E-dipping nappe contact at the eastern side of Mt. Kerketas, the top-E kinematic indicators (asymmetric strain shadows around $albite_3$ and $garnet_3$, quartz-c-axis fabrics) (Bernet 1995; Laws 1996) and the geometry of the Miocene graben that occurs about 1 km above the nappe contact indicates that top-E transport is due to extensional faulting. Since post-blueschist-facies metamorphism shows no major discontinuities across the Kerkis and Ampelos thrusts and within the overlying Ampelos nappe (Chen 1992), the cummulative throw during extensional reactivation of the Kerkis thrust and along small-scale normal shear zones within the Ampelos nappe is considered to be less than about 1-2 km. D_3 kinematic indicators away from this nappe contact yielded alternating top-E and top-W shear sense. Microprobe work on the minerals in D_3 strain shadows shows that D_3 structures started to develop during and closely after the peak of M_3 metamorphism.

The extensional structures are in turn overprinted by contractional structures (D_4), such as upright to W-vergent folds, reverse faults and top-W displacing thrusts (Fig.1). Weidmann et al. (1984) constrained this event between 8-10 Ma. Contractional deformation caused a major change in the sedimentary facies pattern; lacustrine deposits were replaced by conglomerates suggesting that contraction was associated with pronounced uplift. After about 8 Ma, extensional faulting revived (D_5) and continues until the present.

5. VERTICAL DUCTILE THINNING

To quantify the degree of ductile thinning of the overburden of the high-pressure rocks, finite strain and the mean kinematic vorticity number, W_m, have been estimated. Finite strain was assessed from the shape of deformed feldspar augen in orthogneiss, the outlines of chloritoid porphyroblasts in kyanite-chloritoid schist and the grain shape of deformed quartz grains. The albite, chloritoid and quartz grains yield a strain ratio of $X/Z = 5.8-4.5$ ($=R_f$). Since all of these minerals are recrystallised, these estimates are

probably best considered to be minimum values. Another indication of finite strain is provided by the angle between fold axes and the stretching lineation. Throughout the region of distributed shear, this angle does not exceed 10° whereas it is on the order of 45°-60° in intervening low-strain areas. The change in angle indicates a strain increase of $R_f \geq 5.5$. W_m has been estimated from the orientation of the long axes of albite and chloritoid porphyroblasts of different aspect ratios with the mesocopic foliation in zones of distributed shear (Fig.3) (Passchier 1988). The plots in Fig.3 suggest W_m of about 0.88. Wallis (1992) used the angle between the central girdle of quartz c-axis diagrams and the flattening plane of strain, b, to estimate W_m. Quartz c-axis diagrams from 26 samples (Bernet 1995; Laws 1996) have yielded $2° < b < 23°$, which yields a huge range for W_m of $0.21 < W_m < 0.98$. The mean for W_m as deduced from the quartz c-axis patterns is 0.68.

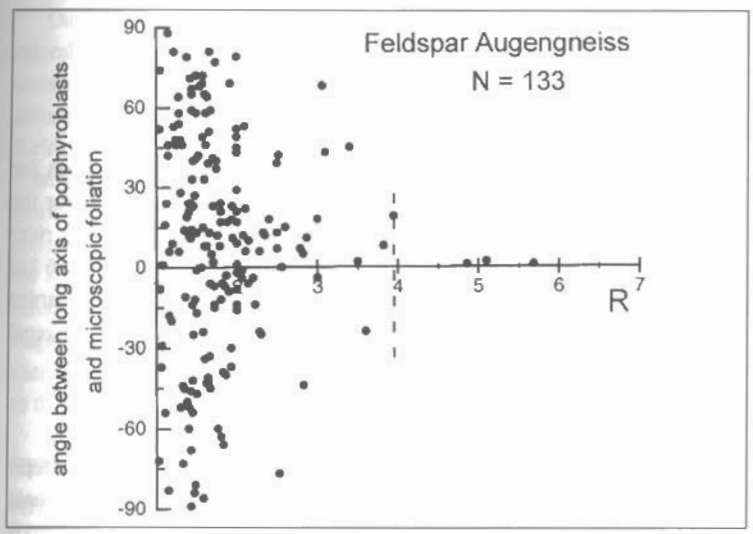

Fig. 3: Aspect ratio, R, plotted against angle between long axis of porphyroblasts and penetrative foliation. Plots are shown for albite porphyroblasts in feldspar augengneiss from Samos Isalnd. The dashed line defines critical aspect ratio, R_C, which divides clasts whose long axes reached a stable position subparallel to the foliation and those with lower aspect ratios that did not find a stable position and thus show a large scatter in readings. Since this change occurs, deformation deviated from simple shear and caused thinning in the vertical. The inferred R_C suggests W_m of about 0.88

The amount of vertical shortening can be calculated using a Mohr circle construction. Assuming steady-state flow and isochoric deformation and using a value of $R_f = 5$ and $W_m = 0.9$ provides a bulk vertical shortening of 33% (Fig.4).

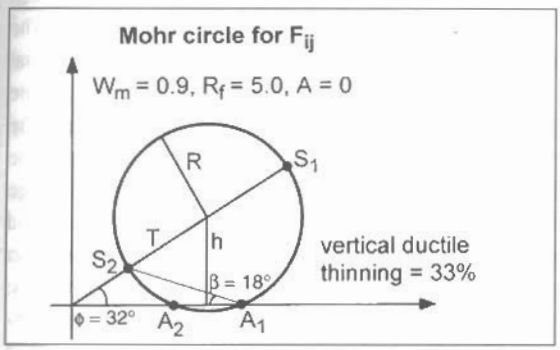

Fig. 4: Mohr-circle construction showing angle between flow plane (foliation) and axes of finite strain in stretch space. T = distance from the origin to centre of circle, h = distance of centre of circle above horizontal axis, R = radius of circle. W_m, R_f and assumed dilatancy number, A, are shown above Mohr circle. Calculated amount of vertical ductile thinning is 33%.

This value is considered a minimum estimate. W_m less than 0.9 and/or deformation-related volume loss would yield an estimate higher than 40%. To properly estimate the contribution that vertical ductile thinning made to the total exhumation of the blueschists, we need to consider both the vertical rate at which the rocks moved through the wedge and the rate of thinning of the remaining overburden at each step along the path. For this purpose, we use a numerical model which models exhumation and ductile strain for a particle moving through a steady—state wedge (Feehan 1997). To model vertical ductile thinning, we need t[illegible] greenschist-facies conditions

lasted at least until about 16 Ma suggesting that subgreenschist-facies conditions in the blueschists were not reached much before 10 Ma. This suggests that the blueschists were in the ductile field for about 40 Ma. The depth of the brittle-ductile transition in the *Blueschist Unit* probably has been lifted up during exhumation and we envision it to be at 10 km depth. The model calculations are based on a ductile-strain-rate law that is proportional with depth and indicate that ductile thinning contributed about 23% or ~12 km to the overall exhumation.

Table 1. Orogenic parameters

Principal Streches (X : Y : Z)	2.07 : 1 : 0.48
Mean Kinematic Vorticity Number	0.8
Depth of Accretion	50 km
Depth of Brittle-Ductile Transition	10 km
Residence Time in Ductile Regime	40 Ma

6. EROSION

Ahnert (1970) formulated a functional relationship between topography and rates of erosion for temperate regions. Applying this approach yields a present-day erosion rate of about 0.2 mm/a for the study area. Westaway (1994) calculated a long-term erosion rate of up to 0.2 mm/a from the river discharge in the Menderes Massif. A rate of 0.2 mm/a yields a total erosional denudation of about 6 km since the proposed onset of horizontal extension in mid-Oligocene times. This estimate has to be regarded as a minimum estimate because relief and erosion rate might have been greater during earlier orogenic events when higher topography may have been present.

7. EXHUMATION

In broad terms, the exhumation history of the *Blueschist Unit* can be separated into two general steps: (1) 25 km of syn-contraction exhumation between ~50 Ma and 30 Ma; and (2) 25 km of syn-extensional exhumation between 30 Ma and 0 Ma. Since the steep increase in metamorphic pressure across the Kerkis thrust was created before the M_3 greenschist-facies overprint, we propose that this break is due to thrusting of the Ampleos nappe on top of the Kerketas nappe. Accordingly, the greenschist-facies overprint in the Kerketas nappe is due to tectonic loading by the advancing blueschist-facies nappes. Because the Kerketas nappe only shows a greenschist-facies overprint, the *Blueschist Unit* must have been reduced in thickness by about 20-30 km before final emplacement on top of the Kerketas nappe. The simultaneous contractional deformation in the cover (Lycian nappes) indicates that no extensional structures were active in the Eocene and Early Oligocene. Consequently, thickness reduction in the *Blueschist Unit* during this stage was apparently due to erosion and vertical ductile thinning. From the strain data above, we conclude that that the 25 km of exhumation during the contractional phase can be factorized into about 9-10 km due to vertical ductile thinning and ~15-16 km due to erosion at an average rate of ~0.8 mm/a. Eocene and Early Oligocene thrusting of the *Blueschist Unit* on top of a cold foreland unit coupled with erosion caused rapid cooling and decompression of the blueschists (Fig.2). Exhumation of the remaining 25 km during horizontal extension since mid Oligocene time can be separated as follows: (*i*) Omission of section underneath the ophiolite nappe and above the Kerketas nappe suggests about ≤15-16 km of extensional denudation; (*ii*) ~2-3 km due to vertical ductile thinning; and (*iii*) contributed another >6 km due to erosion. We consider these estimates to be accurate within ±20%. The estimates for erosion and vertical ductile thinning are minimum values whereas the amount for exhumation by horizontal extension is a maximum estimate.

Our first-order calculations suggest that erosion was the major player that contributed to the exhumation of the Aegean blueschists exposed on Samos Island. The average erosion rates reported herein are moderate, but indirectly inferred. In general, erosion is a function of roughness (Ahnert 1970) which is in turn dominantly controlled by maximum elevation (Hay et al. 1988). The climate for the Eocene and

Oligocene in the northeastern Tethys was in general subtropical and temperate (Prothero & Berggren 1992). The barometric data suggest that the crust in the Eocene was at least 50 km thick. Assuming that the amount of time needed for the geomorphic system to reach steady state was short, crustal thickening should have produced an average elevation of a couple of kilometers. Increased elevation in temperate regions should have resulted in increased erosion rates. Paleogene sediments are widespread and voluminous, especially in the foreland units to the south (Pindos and Westhellenic units). They include the Pindos flysch (Seidel 1971), parts of the Phyllite series on the Peloponnes (Lekkas & Ioakim 1981) and the upper parts of the Plattenkalk series (Jacobshagen 1986).

8. CONCLUSIONS

Our calculations are approximate, but they indicate some interesting conclusions: (1) Exhumation typically occurs by multiple processes. (2) Erosion was the major agent that exhumed the blueschists on Samos Island. Therefore this study provides another example demonstrating that erosion is an efficient exhumation process and commonly plays a major role. (3) About 50% of the overall exhumation occurred during horizontal crustal contraction. This demonstrates pronounced crustal shortening along the exhumation path. (4) Because the time span for contractional deformation (~20 Ma) was shorter than the span for horizontal extension (~30 Ma), average exhumation rates during crustal shortening were generally higher than during crustal extension. (5) Since subhorizontal thrusting of the *Blueschist Unit* onto the Kerketas nappe was characterized by a degree of noncoaxiality less than simple shear, thrusting was associated by subvertical ductile thinning which contributed about 40% to the total exhumation during this stage. (6) Retrograde metamorphism during decompression was caused by thrusting of the *Blueschist Unit* onto the cold foreland. (7) During overall horizontal crustal extension normal faulting contributed ≤60% to the overall exhumation of the Samos blueschists.

REFERENCES

AHNERT, F. 1970, Functional relationships between denudation, relief, and uplift in large mid-latitude drainage basins: Am. J. Sci., 268, 243-263.

ALTHERR, R., SCHLIESTEDT, M., OKRUSCH, M., SEIDEL, E., KREUZER, H., HARRE, W., LENZ, H., WENDT, I. & WAGNER, G.A. 1979, Geochronology of high-pressure rocks on Sifnos (Cyclades, Greece): Contrib. Mineral. Petrol., 70, 245-255.

AVIGAD, D. & GARFUNKEL, Z. 1991, Uplift and exhumation of high-pressure metamorphic terrains: the example of the Cycladic blueschist belt (Aegean Sea): Tectonophysics, 188, 357-372.

BERNET, M. 1995, Zur regionalen Geologie südwestlich von Karlovassi, Samos, Griechenland: Unpubl. mapping report, Univ. Mainz, 43 pp.

BRANDON, M.T. & RING, U. 1997, Exhumation processes: Normal faulting, ductile flow, and erosion: GSA Today, 7 (5), 17-20.

BUICK, I.S. 1991, The late-Alpine evolution of an extensional shear zone, Naxos, Greece: J. Geol. Soc. Lond., 152, 639-654.

CHEN, G. 1992, Evolution of the high- and medium-pressure metamorphic rocks on the island of Samos, Greece: Unpubl. Ph.D. thesis, Univ. Würzburg, 170 pp.

COLLINS, A.S. & ROBERTSON, A.H.F. 1997, Lycian melange, southwestern Turkey: An emplaced Late Cretaceous accretionary complex: Geology, 25, 255-248.

ERDOGAN, B. & GÜNGÖR, T. 1992, Menderes Masifi'nin kuzey kanadinin stratigrafisi ve tektonik evrimi: TPJD Bületeni, 2, 1-20.

FEEHAN, J.G. 1997, Finite Strain and Fluid Flow in Accretionary Wedges, NW Washington State: Unpubl. Ph.D. thesis, Yale University.

HAY, W.W., SHAW, C.A. & WOLD, C.N. 1989, Balanced paleogeographic maps: Geol. Rdschau, 78, 207-242.

JACOBSAHGEN, V. 1986, *Geologie von Griechenland*, Gebrüder Borntrüger, Berlin, 363p.

JANSEN, J.H.B. 1977, The geology of Naxos: Geol. Geofy. Meletai, 19, 100 p.
KATSIKATSOS, G. 1977, La structure tectonique d'Attique et d'ile d'Eubee: Proceedings 6th Colloq. Geol. Aegean Region (Athens), p.211-228.
LAWS, S. 1996, Die tektonische Entwicklung der Insel Samos (östliche Ägäis): Unpubl. Diploma thesis, Univ. Mainz, 85 pp.
LEKKAS, S. & IOAKIM, C. 1981, Données nouvelles sur l'age des phyllades en Péloponnüse central (Grüce): Prakt. Akad. Athinon, 55, 350-361.
LISTER, G.S., BANGA, G. & FEENSTRA, A. 1984, Metamorphic core complexes of Cordilleran type in the Cyclades, Aegean Sea, Greece: Geology, 12, 221-225.
MPOSKOS, E. & PERDIKATSIS, V. 1984, Petrology of glaucophane metagabbros and related rocks from Samos, Aegean Island: N. Jahrb. Mineral. Abh., 149, 43-63.
PAPANIKOLAOU, D. 1979, Unités tectoniques et phases de déformation dans l'île de Samos, Mer Egée, Grüce: Bull. Soc. Geol. Fr., 21, 745-752.
PASSCHIER, C.W. 1988, Analysis of deformation path in shear zones: Geol. Rdschau, 77, 309-318.
PROTHERO, D.R. & BERGGREN, W.A. 1992, Eocene-Oligocene climatic and biotic evolution. Princeton University Press, 568 pp.
RIDLEY, J. 1984, The significance of deformation associated with blueschist-facies metamorphism on the Aegean island of Syros: Geol. Soc. Lond. Spec. Publ., 17, 545-550.
SEIDEL, E. 1971, Die Pindos-Serie in Westkreta, auf der Insel Gavdos und im Kedros-Gebiet (Mittelkreta): N. Jahrb. Geol. Paläont. Abh., 137, 443-460.
SEIDEL, E., OKRUSCH, M., KREUZER, H., RASCHKA, H. & HARRE, W. 1981, Eo-Alpine metamorphism in the uppermost unit of the Cretan nappe system - petrology and geochronology. Part 2. Synopsis of high-temperature metamorphics and associated ophiolites: Contrib. Mineral. Petrol., 76, 351-361.
THEODOROPOULOS, D. 1979, Geological map of Greece, 1:50000. Samos Island: I.G.M.E., Athens.
WALLIS, S.R. 1992 Vorticity anaylsis in a metachert from the Sanbagawa Belt, SW Japan: J. Struc. Geol, 14, 271-280.
WEIDMANN, M., SOLOUNIAS, N., DRAKE, R.E. & CURTIS, G.H. 1984, Neogene stratigraphy of the eastern basin, Samos island, Greece: Geobios, 17, 477-490.
WESTAWAY, R., 1994, Evidence for dynamic coupling of surface processes with isostatic compensation in the lower crust during active extension of western Turkey: J. Geophys. Res., 99, 20203-20223.
WIJBRANS, J.R., SCHLIESTEDT, M. & YORK, D. 1990, Single grain argon laser probe dating of phengites from the blueschist to greenschist transition on Sifnos (Cyclades, Greece): Contrib. Mineral. Petrol., 104, 582-593.